

**MINISTRY OF EDUCATION  
AND TRAINING**

**VIETNAM ACADEMY OF SCIENCE  
AND TECHNOLOGY**

**GRADUATE UNIVERSITY OF SCIENCE AND TECHNOLOGY**

-----



**NGUYEN THI LIEU**

**RESEARCH ON THE SYNTHESIS OF NANOMAGNETIC  
MATERIALS AND GRAPHENE OXIDE COMBINED  
COPOLYMER AM-NVP/AM-PVP FOR APPLICATION  
IN ENHANCE OIL RECOVERY AT HIGH  
TEMPERATURE OFFSHORE RESERVOIRS**

**SUMMARY OF DISSERTATION ON CHEMISTRY  
DOCTORAL THESIS POLYMERS AND COMPOSITE  
MATERIALS**

**Code: 9440125**

**Ha Noi - 2024**

The dissertation is completed at: Graduate University of Science and Technology, Vietnam Academy Science and Technology

Supervisors:

Supervisor 1: Assoc. Prof. Dr. Nguyen Phuong Tung

Supervisor 2: Dr. Nguyen Hoang Duy

Referee 1: Assoc. Prof. Dr. Nguyen Tran Ha

Referee 2: Assoc. Prof. Dr. Nguyen Anh Tien

Referee 3: Dr. Nguyen Huu Luong

The dissertation is examined by Examination Board of Graduate University of Science and Technology, Vietnam Academy of Science and Technology at 01A, Thanh Loc 29, Thanh Loc ward, 12 District, Ho Chi Minh City.

At ..... hour..... date..... month .....202.

The dissertation can be found at:

1. Graduate University of Science and Technology Library
2. National Library of Vietnam

## INTRODUCTION

**1. The necessity of the thesis:** With current oil and gas exploitation techniques, after the primary and secondary exploitation stages, a large amount of oil remains in the porous, cracked structure of the reservoir rock. Therefore, the research and development of materials used in enhanced oil recovery (EOR) attracts the attention of many researchers to increase the oil recovery rate. Injection of nanofluids and polymer solutions has been proven to be an effective EOR method because of characteristics such as changing the mobility ratio, changing the wettability and reducing the interfacial tension. Polymer coated magnetic nanoparticles and graphene oxide (GO) grafted polymer have also been proven to be materials that can increase the oil recovery coefficient, and are highly feasible and effective in EOR

**2. Objectives of the thesis:** Synthesis of polymer-coated magnetic iron oxide nanomaterials (PMNPs) and GO-Polymer materials (GO-P(AM-NVP), GO-P(AM-PVP) for application in EOR at Miocene and Oligocene reservoirs of Bach Ho field, Vietnam.

**3. Research scope and content:** Contributing new nanomaterials have cost-effective: PMNPs, GO-P(AM-NVP) and GO-P(AM-PVP) have significance to find cost-effective that can withstand high temperatures, high salinity of brine has potential in practice as an injection agent in EOR in Vietnam's offshore.

**4. Structure of the thesis:** The dissertation has 132 pages, including the Preface, Chapter 1: Overview, Chapter 2: Experiment, Chapter 3: Results and discussions, Conclusions, publications with 56 images, 37 tables and 145 references.

### Chapter 1. OVERVIEW

EOR is the process of introducing foreign agents that have not yet present

in the oil reservoir to change the properties of the fluid and reservoir rocks. Methods used in this stage such as surfactant injection, alkali injection, polymer injection or nanofluid injection help increase the fluidity of oil to increase exploitation output. Currently, the synthesis and modification of nanomaterials that can withstand harsh reservoir conditions for application as injection agents attracts much research attention.

Polymer-coated magnetic iron oxide nanomaterials with a core-to-core structure are used in EOR because the special properties of nanomaterials such as they can self-arrange to change the adhesion of reservoir rocks from lipophilic to hydrophilic water and reduces the interfacial tension between the two oil-water phases. In addition, the outer shell is made of heat-stable polymers that can withstand harsh reservoir conditions such as high temperature and high salt of brine.

The most commonly used synthetic polymers in the polymer injection process in EOR are polyacrylamide (PAM) and partially hydrolyzed polyacrylamide (HPAM). However, HPAM/PAM is easily hydrolyzed in high temperature environments and in the hardness and high salinity of sea water. To protect HPAM/PAM from hydrolysis as influenced by temperature and divalent ion content, modification of their structure with different monomers has been widely studied. Meanwhile, NVP can effectively protect AM groups from high-temperature hydrolysis due to the presence of the 5-lactam-pyrrolidone ring in the copolymer.

The use of polymerization by  $\gamma$ -ray irradiation is of interest in research. Because this method has outstanding advantages such as being able to create diverse, high-quality polymers that are soluble in salt water and thermally stable, it is easy to scale up for offshore applications.

Based on the properties of this material, we propose to research the synthesis of polymer-coated magnetic iron oxide nanomaterials (PMNPs)

and polymer-grafted GO materials (GO-P(AM-NVP) and GO-P(AM- PVP) by gamma ray irradiation applied in EOR in high-temperature offshore oil reservoirs such as Miocene and Oligocene Bach Ho field, Vietnam.

## Chapter 2. EXPERIMENT

### 2.1. Synthesis of polymer-coated magnetic nanomaterials-PMNPs

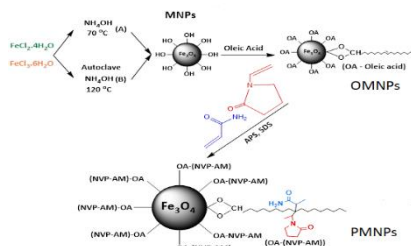


Figure 2.1. The synthesis process PMNPs

The characteristics of PMNPs was determined analysis methods such as XRD, FT-IR, TEM, DLS, VSM, TGA, XPS. The possibility of applying EOR has been evaluated through methods such as determining thermal stability, chemical stability, the ability to change wet adhesion and reduce surface tension.

### 2.2. Synthesis of GO-Polymer

#### 2.2.1. Synthesis of GO-P(AM-NVP)

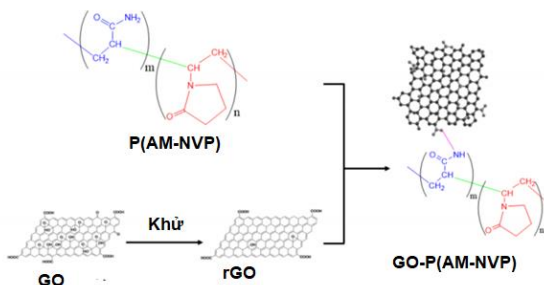
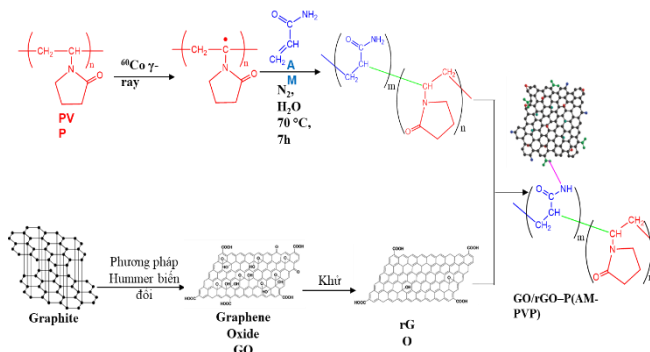


Figure 2.2. The synthesis process of GO-P(AM-NVP)

Factors affecting the synthesis of P(AM-NVP) such as  $\gamma$ - ray irradiation dose, monomer concentration as well as optimal polymerization process to create AM-NVP copolymer were investigated through experimental planning and stargraphic software. The characteristics of GO-P(AM-NVP) was by analysis methods such as FT-IR, Raman, SEM, SEM-EDX, XPS.

### 2.3. Synthesis of-GO-P(AM-PVP)



*Figure 2.3. The synthesis process GO-P(AM-PVP)*

Factors affecting the synthesis of P(AM-NVP) such as  $\gamma$ - ray irradiation dose, monomer concentration as well as optimal polymerization process to create AM-NVP copolymer were investigated through experimental planning and stargraphic software. The characteristics of GO-P(AM-NVP) was by analysis methods such as FT-IR, Raman, SEM, SEM-EDX, XPS.

### 2.4. Evaluate the applicability in EOR of materials

The possibility application in EOR of PMNPs has been evaluated by evaluating the change in the contact angle of reservoir rock and the reduction of interfacial tension between the two oil-water phases. In addition, the thermal stability and chemical stability of the materials PMNs, GO-P(AM-NVP), and GO-P(AM-PVP) have been assessed for EOR application in high-

temperature offshore reservoirs through measurements of the viscosity of the solution after annealing at temperatures of 120°C and 135°C.

### Chapter 3. RESULTS AND DISCUSSIONS

#### 3.1. PMNPs composite

##### 3.1.1 The characteristics of PMNPs

The surface structure of PMNPs and OMNPs was studied through Fourier transform infrared spectroscopy (FT-IR). The phase composition and crystal structure of MNPs and PMNPs materials were determined by X-ray diffraction method.

The FT-IR spectrum of PMNPs (Fig 3.1 Bb) in the wave region 1600-1500  $\text{cm}^{-1}$  almost does not show the characteristic peak of C=C. This proves that the copolymerization reaction is carried out completely left and there is no residual monomer. The appearance of characteristic peaks of stretching vibrations of the -NH- and C=O bonds of AM in the wave region 3200-3100  $\text{cm}^{-1}$  and 1750-1700  $\text{cm}^{-1}$ .

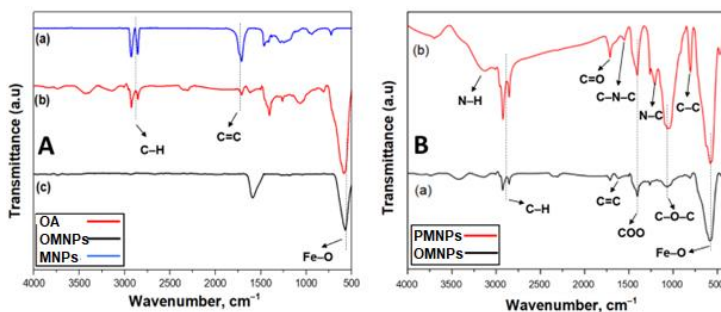


Figure 3.1. FT-IR spectrum of PMNPs

There are also characteristic peaks of NVP appearing in the wave region of 1550-1500  $\text{cm}^{-1}$  (stretching vibration of the C-N-C bond), 1250-1200  $\text{cm}^{-1}$  (stretching vibration of the C-N bond) and 850-800  $\text{cm}^{-1}$  (stretching vibrations of the C-C bond). This proves that AM and NVP were successfully coated on MNPs and PMNPs was successfully synthesized.

Fig. 3.2 is the X-ray diffraction pattern of MNPs, OMNPs and PMNPs materials with MNPs synthesized by co-precipitation method (A) and hydrothermal method (B).

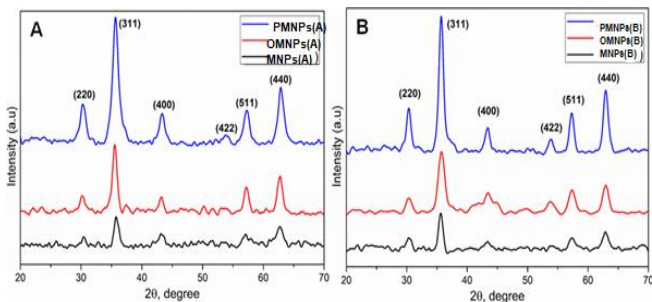


Figure 3.2. X-ray diffraction pattern of PMNPs

The crystalline characteristics of  $\text{Fe}_3\text{O}_4$  are shown at the angles  $2\theta = 30.3^\circ, 35.6^\circ, 43.3^\circ, 53.9^\circ, 57.5^\circ$  and  $62.9^\circ$  corresponding to the (220), (311), (400), (422), (511), (440) planes. This proves that MNPs have been successfully synthesized and it can be seen that the two synthesis methods are different but the structure of the material does not change. The relative crystallite size of  $\text{Fe}_3\text{O}_4$  in MNPs and PMNPs was calculated through the Scherrer equation at the diffraction peak  $2\theta = 35.6^\circ$  as 12nm and 11nm, respectively.

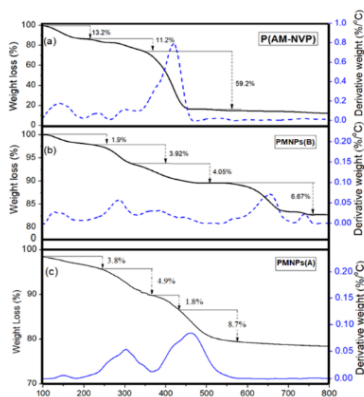


Figure 3.3. TGA results of PMNPs



Fig. 3.3 is the TGA results of PMNPs and P(AM-NVP). The results show that the copolymer has three stages of mass loss at 160°C, 330°C and 450°C. After 450°C, the remaining copolymer mass is about 16.4%. PMNPs have four stages of mass loss at 180°C, 310°C, 540°C and 740°C. After 740°C, the remaining material mass is about 81%. The presence of P(AM-NVP) in the structure of the nanocomposite material leads to a higher decomposition temperature. Shows that MNPs materials do not change too much at high temperatures. The main mass loss is due to the mass loss of the copolymer. The mass percentage of copolymer coated into MNPs can be estimated at about 10.7%, which proves that AM-NVP copolymer has been coated into the MNPs material.

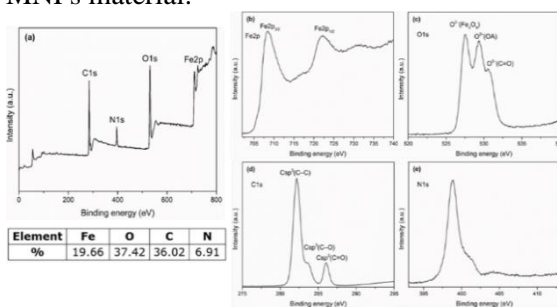


Figure 3.4. XPS spectra of PMNPs

The XPS spectrum of PMNPs material shows the chemical state and electronic state of the elements in Fig. 3.4. The results show the presence of elements Fe2p, O1s, N1s, C1s. That proves the presence of four elements, Fe, O, N, C. The spectral bands of O1s are assigned to the oxygen anion ( $O^{2-}$ ) in  $Fe_3O_4$ , in oleic acid and the C=O bond of NVP and AM. The spectrum of C1s shows the presence of  $sp^2$  hybridized C in the C-C, C-O bonds of oleic and C=O of NVP and AM. The spectral range of N1s is related to  $N^{3-}$  in the structure of AM and NVP.

### 3.1.2. Morphological characteristics and particle size distribution of PMNPs

The morphology and particle size of PMNPs were analyzed through transmission electron microscopy (TEM) and dynamic light scattering (DLS)

Figure 3.5 shows TEM images of MNPs and PMNPs. It is seen that  $\text{Fe}_3\text{O}_4$  particles without polymer coating do not disperse well and easily agglomerate (Figure 3.5 a and c). The particles are spherical with average size of 12 nm. When coated with polymer to form PMNPs, the particles have average size of 16nm, spherical shape, well dispersed (Figure 3.5 b and c).

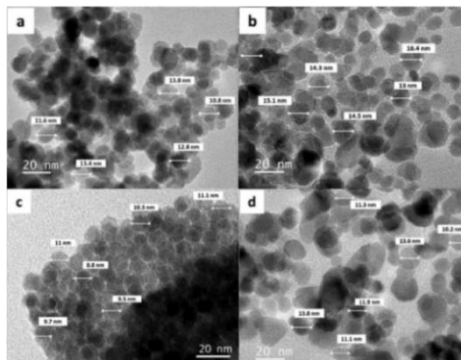


Figure 3.5. TEM images of MNPs and PMNPs

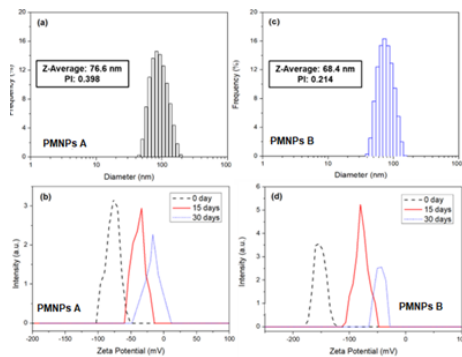


Figure 3.6. Particle size distribution and zeta potential of PMNPs in brine

Figure 3.6 shows the DLS results and zeta potential of PMNPs in brine. The results show that the hydrodynamic size distribution of PMNPs in brine is 40-130nm, average size is 68nm, PI index = 0.214, proving that the material is monodisperse. In addition, the high negative zeta potential value of the PMNPs before and after annealing at 120°C for 15 days also shows the stable dispersion ability of the material.

### 3.1.3. Magnetic characteristics of PMNPs

The magnetization of the material is shown through the measurement results of the vibrating sample magnetometer as shown in Figure 3.7:

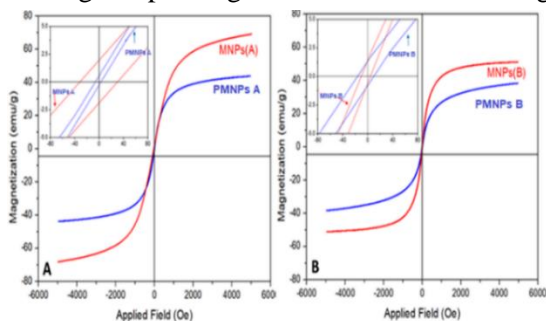


Figure 3.7. VSM results of MNPs and PMNPs

Figure 3.7 is the VSM results of MNPs and PMNPs materials. The bare MNPs have a saturation magnetization of 53 emu/g and 69 emu/g. The PMNPs particles have saturation magnetization of 42 emu/g and 39 emu/g. The results show that there is a decrease in the magnetization of the material after coated polymer, which is explained by the fact that the magnetic effect is proportional to the magnetic effect present in the material. In addition, the coercivity and remanence of the MNPs and PMNPs materials are 35.2; 38.1 and 2.9 and 4.4 emu/g; respectively demonstrate that the two materials have similar magnetic properties, indicating that the superparamagnetism of the material is well maintained after coated polymer.

### 3.1.4. Optimization of the polymerization reaction

The process of coated AM-NVP into MNPs material is optimized according to the percentage of polymer coated. The results in Fig. 3.8 show that at temperature of 70°C and reaction time of 8 hours, the amount of polymer coated into MNPs is the highest at 11.04%.

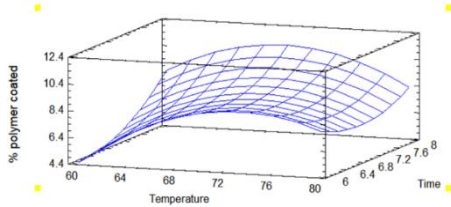


Figure 3.8. Response surface % AM-NVP coated on MNPs

### 3.1.5. Evaluate the applicability of PMNPs in EOR

#### 3.1.5.1. Evaluation of thermal and chemical stability of PMNPs nanofluids

Stability at high temperatures is one of the important factors when applying PMNPs in reservoir environments. Therefore, determining the thermal stability of PMNPs nanocomposite materials by thermal annealing method is necessary to evaluate its degradation properties especially in EOR. According to the technical requirements of VietsoPetro, the incubation time at reservoir temperature is 31 days. The appearance and viscosity of PMNPs during the annealing process are shown in Figure 3.9 below:

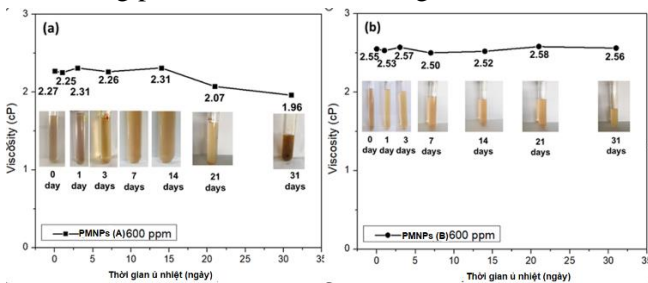


Figure 3.9. Viscosity and appearance of PMNPs A annealing at 120 °C (a) and of PMNPs B annealing at 135 °C (b)

Fig. 3.9 shows that the 600ppm PMNPs nanofluid solution in the thermal annealing test gave good results at 135°C for 31 days with almost unchanged viscosity and appearance, proving that the dispersions are thermally and chemically stable under static conditions similar to in the Miocene and Oligocene mines of Bach Ho field.

### 3.1.5.2. Evaluate the ability of PMNPs solution to change the wettability of reservoir rock and reduce the interfacial tension

The results of contact angle and IFT measurements of PMNPs solution are shown in table 3.1 and Fig. 3.10 below:

*Table 3.1. Effects of changing the contact angle IFT of PMNPs solution at different concentrations*

Concentration PMNPs (ppm)	Proportion	Viscosity (cP)	Contact angle (°)	IFT(Nn/m)
0	1.026	-	27	62.53
200	1.026	2.23	78	48.25
400	1.026	2.24	86	42.87
600	1.027	2.43	93	32.87
800	1.027	2.54	103	24.53
1000	1,027	2.55	126	12.64

Regardless of the PMNPs concentration, the contact angle of the oil droplet on the sandstone surface of Bach Ho field in the diluted PMNPs nanofluid was always higher than the contact angle observed in the simulated seawater solution for found the positive impact of polymer-coated magnetic nanomaterials in changing the sandstone surface from hydrophobic to hydrophilic.

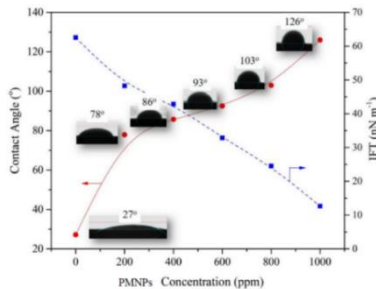


*Figure 3.10. Effect of PMNPs concentration on contact angle and IFT*

### 3.2. Synthesis of GO-P(AM-NVP)

#### 3.2.1. Effect of irradiation dose on reaction efficiency to create P(AM-NVP) copolymer

Conduct irradiation at doses of 2, 5, 10, 15Kgy. As a result, when irradiated at a dose of 5Kgy, the copolymer product dispersed well in seawater and had the highest viscosity. Product P(AM-NVP) is shown in Fig.3.11:

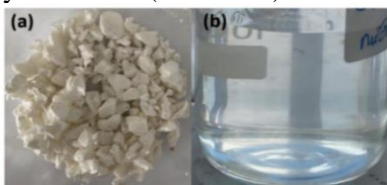


*Figure 3.11. P(AM-NVP) after refined (a) and when dispersed in brine (b)*

#### 3.2.2. The effects of ingredients and monomer concentration on product performance and molecular weight of copolymer

The results of survey at molar ratios AM/NVP 4/5; 1/1; 3/1; 2/1 at concentrations of 15, 20, 25%. The results show that product yield and molecular weight are stable at AM/NVP molar ratio 2/1 and monomer concentration 20%.

#### 3.2.3. Optimization of the P(AM-NVP) copolymer synthesis process

The P(AM-NVP) copolymer synthesis process is optimized according to the viscosity of the copolymer solution. The results in Fig.3.12 show that at AM/NVP molar ratio of 1.71 and monomer concentration is 23.19%, the 0.5% P(AM-NVP) solution in brine is obtained with the highest viscosity is 5.02 cP matches the viscosity of crude oil.

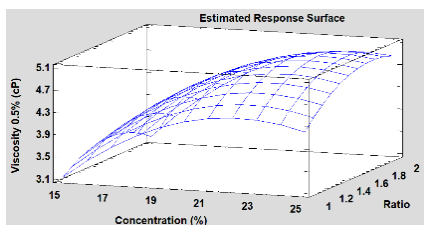


Figure 3.12. Viscosity response surface of 0.5 wt% copolymer solution

### 3.2.4. Physical and chemical characteristics of GO-P(AM-NVP)

#### 3.2.4.1. FT-IR spectrum of the material

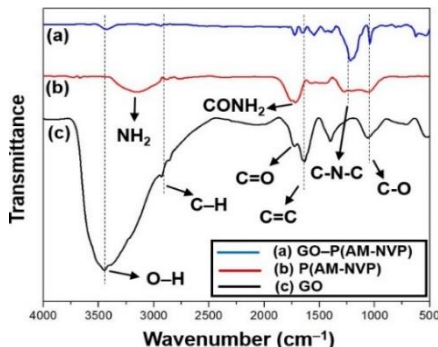


Fig. 3.13. FT-IR spectrum of GO-P(AM-NVP) (a), P(AM-NVP) (b), GO(c)

FT-IR spectra of GO-P(AM-NVP), P(AM-NVP) and GO confirm the presence of P(AM-NVP) on GO shown in Fig. 3.13. The FT-IR spectrum of GO-P(AM-NVP) has peaks appearing in the wave bands at  $3450\text{--}3350\text{ cm}^{-1}$  corresponding to the stretching vibration of the O-H group of GO. The peaks observed at  $2900\text{--}2800\text{ cm}^{-1}$  and  $1090\text{--}1110\text{ cm}^{-1}$  are related to the stretching vibration of the  $\text{Csp}^3\text{-H(-CH}_2\text{-)}$  bond and the stretching vibration of the C-O group. The peaks appearing in the waveband  $1660\text{--}1650\text{ cm}^{-1}$  characterize the C=O bond observed in AM. In addition, the peaks appearing in the wave range  $1320\text{--}1293\text{ cm}^{-1}$  in the FTIR spectrum of GO-P(AM-NVP) and P(AM-NVP) are asymmetric stretching vibrations of the C-N-C group of the rings of NVP proves that NVP has been successfully grafted on this material. In particular, the peaks appearing in the wavebands  $1550\text{--}1500\text{ cm}^{-1}$  of the GO-P(AM-NVP) FTIR spectrum correspond to the stretching vibrations of the N-O bond. These bonds were formed between copolymer (N) and GO (O), confirming P(AM-NVP) was covalently bonded to GO.

#### 3.2.3.2. Raman spectrum of GO-P(AM-NVP)

Fig.3.14 is the raman spectrum of GO and GO-P(AM-NVP). Characteristic peak of graphene at D band with wavelength  $1361\text{ cm}^{-1}$  of GO and  $1336\text{ cm}^{-1}$  of GO-P(AM-NVP) and at G band with wavelength  $1592\text{ cm}^{-1}$  of GO and  $1582\text{ cm}^{-1}$  of GO -P(AM-NVP) indicates  $\text{sp}^2$  hybridization or C=C bond in the GO structure.

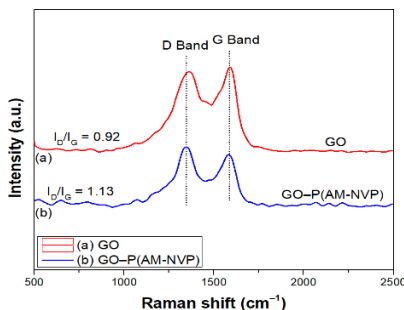


Figure 3.14. Raman spectra of GO and GO-P(AM-NVP)

The  $I_D/I_G$  values of GO and GO-P(AM-NVP) are 0.92 and 1.13, respectively, which shows that copolymer molecules grafted onto GO increase local defects and disorder in GO.

### 3.2.3.3. SEM images of P(AM-NVP) and GO-P(AM-NVP)

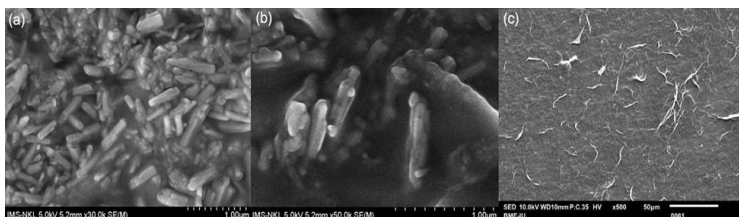


Figure 3.15. SEM images of P(AM-NVP) (a, b) and GO-P(AM-NVP)

Fig. 3.15 is the SEM image of P(AM-NVP) and GO-P(AM-NVP). The P(AM-NVP) has a rod shape (a, b). SEM images also clearly show the morphology of the material with a rod-shaped structure (Figure 3.13 a, b). Fig. c is the SEM image of GO-P(AM-NVP) showing the stable dispersion of polymer (white fiber) on the surface of GO sheet. Proving that the polymer



was successfully grafted onto GO sheets. This result is consistent with the Raman analysis results above. The material surface and elemental composition in GO-P(AM-NVP) were analyzed through the SEM-EDX method shown in Fig. 3.16:

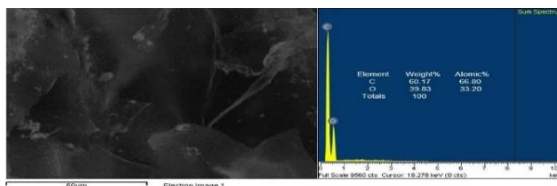


Figure 3.16. SEM-EDX results of GO-P(AM-NVP)

Fig. 3.16 is the result of elemental composition analysis by SEM-EDX of GO-P(AM-NVP). The results showed the appearance of C and O but no N. This can be explained the mass percentage of nitrogen atoms in the two monomers is less than the detection limit of the machine and these monomers are also conjugated to GO-molecules containing many carbon and oxygen atoms.

The elemental mapping image of GO-P(AM-NVP) for O<sub>2</sub>, C and N<sub>2</sub> shown in Fig. 3.17 again shows the relative distribution of nitrogen atoms on the GO surface (Fig. 3.17d) rich and uniform. This SEM elemental mapping result shows that the copolymers were successfully bonded on the GO surface.

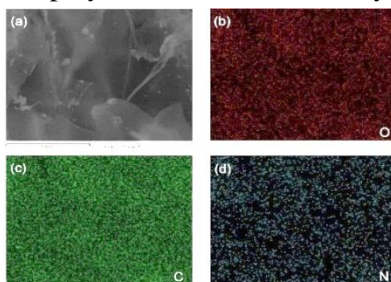


Figure 3.17. SEM mapping image of the fracture structure of GO-P(AM-NVP) (a) of GO-P(AM-NVP); (b) oxygen; (c) carbon; (d) nitrogen

### 3.2.3.4. XPS spectra of GO-P(AM-NVP)

Fig. 3.18 is the XPS result of GO-P(AM-NVP) material. The appearance of the three elements C, N, O is shown through the peaks of C1s, N1s, O1s in the binding energy regions of 285eV, 400eV, 532eV.

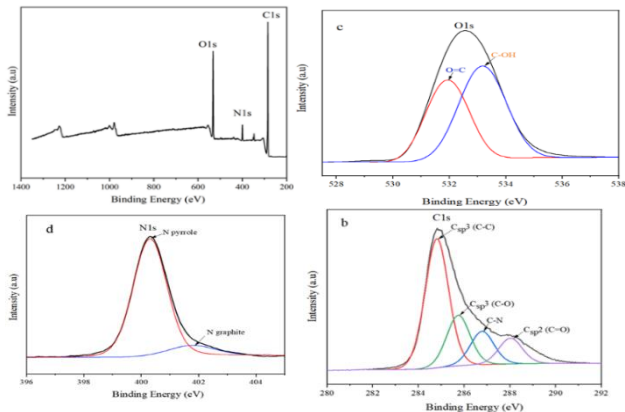


Figure 3.18. XPS spectra of GO-P(AM-NVP)(a) and XPS spectra of C1s(b), O1s(c), N1s(d)







The spectral band of element C1s in GO-P(AM-NVP) is separated into 4 peaks assigned to  $C_{sp^3}$  of the C-C chain,  $C_{sp^3}$  in the C=O bond of NVP and AM. The O1s spectral band is separated into 2 peaks distributed in the bond energy region 531.9eV and 533.2eV assigned to the C=O bond of NVP and AM and HO-C of GO. The spectral band of N1s assigned to pyrrole nitrogen and graphite nitrogen is related to  $N^{3-}$  in NVP and AM.

### 3.2.5. Applicability of GO-P(AM-NVP) in EOR

❖ *Evaluation of thermal and chemical stability of GO-P(AM-NVP) system*

Results of evaluating the thermal stability of the material through annealing test at 135 °C for 31 days. The appearance and viscosity of the system after annealing are shown in table 3.2:

Table 3.2. Appearance and viscosity of GO-P(AM-NVP)1.0 % wt dispersion system

Dispersion system	Annealing time - day / viscosity -cP					
	0	3	7	14	21	31
GO-P(AM-NVP) 1,0 %kl	 4.57	 4.59	 4.56	 4.52	 4.58	 4.55

GO-P(AM-NVP) dispersion system 1.0 % wt dispersed in brine when incubated at 135 °C for 31 days showed almost no change in appearance and insignificant change in viscosity. This proves the possibility of applying the material in EOR.

### 3.3. Synthesis of GO-P(AM-PVP)

#### 3.3.1. Effect of time and irradiation dose on graft polymerization reaction efficiency

The efficiency of the graft polymerization reaction increases as the time and irradiation dose increase. The results are shown in Fig. 3.19. The irradiation dose of 30 KGy gives the highest efficiency, but the product at this irradiation dose is only 40% soluble in brine, so the optimal irradiation dose is 20 KGy.

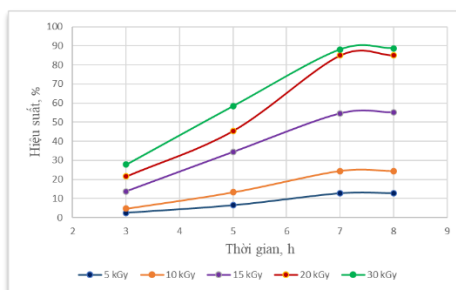


Figure 3.19. Graph showing the effect of time and irradiation dose on reaction efficiency

### 3.3.2. Optimization of the P(AM-PVP) copolymer synthesis process

The efficiency of P(AM-PVP) synthesis was optimized according to reaction time and AM monomer concentration. The highest reaction efficiency reached 85.77% when AM concentration was 19.92% and reaction time was 7.46 h. The surface response performance is as shown in Fig. 3.20:

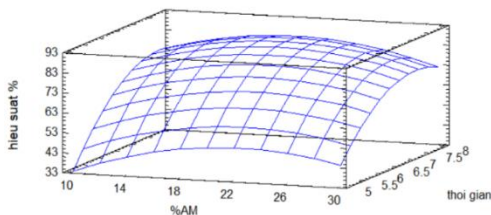


Figure 3.20. Surface response performance of graft polymerization reaction

### 3.3.3. Physicochemical characteristics of GO-P(AM-PVP)

#### 3.3.3.1. FT-IR results of P(AM-PVP) and GO-P(AM-PVP)

FT-IR spectrum of GO-P(AM-PVP) confirms the presence of P(AM-PVP) on GO as shown in Fig. 3.21. The vibrations in the absorption band of wavelength  $1203\text{ cm}^{-1}$  correspond to the asymmetric stretching vibrations of the C-N-C group of the NVP rings, proving the presence of PVP in the material structure. The characteristic absorption bands for the carbonyl group C=O are the stretching vibrations at wavelength  $1660\text{-}1650\text{ cm}^{-1}$  of the P(AM-PVP) and GO-P(AM-PVP) spectra in Fig. 3.21a observed in AM. This proves that AM and PVP have been successfully grafted onto GO.

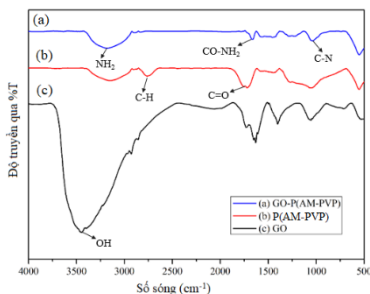


Fig. 3.21. FT-IR spectra of GO-P(AM-PVP) (a), P(AM-PVP) (b) GO (c)

### 3.3.3.2. Raman spectra of GO-P(AM-PVP)

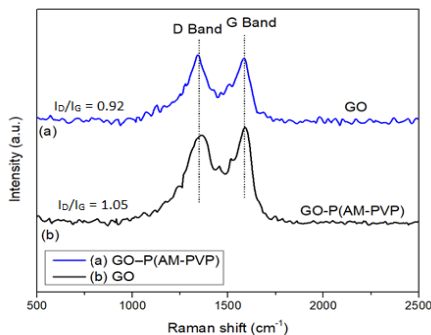


Figure 3.22. Raman spectra of GO and GO-P(AM-PVP)

Fig.3.22 shows the Raman spectra of GO and GO-P(AM-PVP). The characteristic peak of graphene at D band with wavelength  $1360.81\text{ cm}^{-1}$  of GO and  $1339\text{ cm}^{-1}$  of GO-P(AM-NVP) indicates the vibration of  $\text{Csp}^3$  atoms with structural defects and at G band with wavelength  $1591.58\text{ cm}^{-1}$  of GO and  $1585.9\text{ cm}^{-1}$  of GO-P(AM-NVP) is  $\text{Csp}^2$  or  $\text{C}=\text{C}$  bond in GO structure. The results indicate that oxygen functionalization makes GON stable.

The  $I_D/I_G$  values of GO and GO-P(AM-PVP) were 0.92 and 1.05, respectively, which shows that copolymer molecules grafted onto GO increase local defects and disorder in GO. Comparing with the Raman spectrum of GO-P(AM-NVP) in Fig. 3.14, the  $I_D/I_G$  of GO-P(AM-PVP) is lower than that of GO-P(AM-NVP), demonstrating the rate of defects in the graphene structure of GO-P(AM-PVP) is significantly reduced compared to GO-P(AM-NVP).

### 3.3.3.3. Results of thermogravimetric analysis TGA of the material

Fig. 3.23 is the TGA result of P(AM-NVP). The results show that the copolymer has three stages of mass loss at  $108\text{ }^\circ\text{C}$ ,  $302\text{ }^\circ\text{C}$  and  $450\text{ }^\circ\text{C}$ . After  $450\text{ }^\circ\text{C}$ , the remaining copolymer mass is about 16.48%.

The TGA results of GO-P(AM-PVP) in Fig. 3.24 also have three stages of mass loss at 100 °C, 180 °C - 350 °C and 350 °C -450 °C.

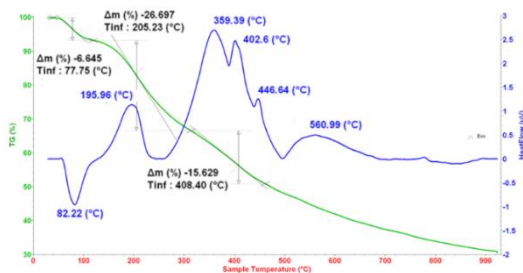


Figure 3.23. The TGA results of P(AM-PVP)

After 450 °C, the remaining material mass about 51%. This result proves that P(AM-NVP) was successfully attached to GO. The copolymer is quite thermally stable at 150 °C. When the temperature reaches nearly 200 °C, there begins to be degradation of the polymer in the material structure, which shows that this material is suitable for application in EOR at the Oligocene mine of Tiger White.

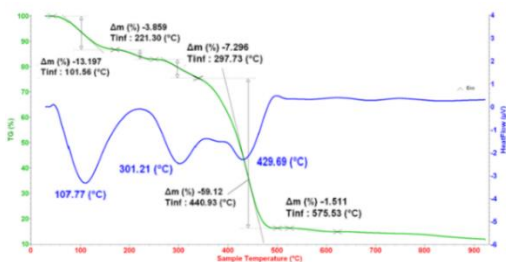


Figure 3.24. The TGA results of GO-P(AM-PVP)

### 3.3.3.4. The results of SEM-EDX and SEM-Mapping

Fig. 3.25 is the SEM image of P(AM-PVP) and GO-P(AM-PVP) showing that the material surface is not smooth but rough. The SEM results of GO-P(AM-NVP) also show that the polymer distribution (AM-NVP) on GO is relatively uniform. The SEM mapping results of GO-P(AM-NVP) in Figure 3.26 show that the density of N on the surface of the material is quite

dense and uniform, proving that the copolymers have been successfully bonded on the GO surface.

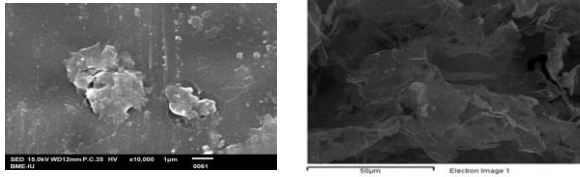


Figure 3.25. The SEM results of P(AM-PVP) and GO-P(AM-PVP)

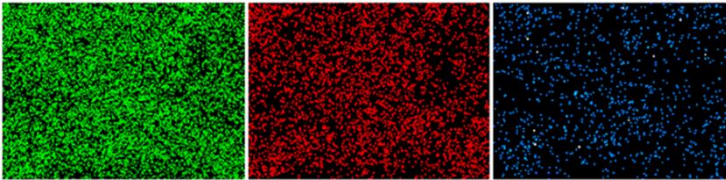


Figure 3.26. SEM mapping results GO-P(AM-PVP)

### 3.3.3.5 XPS spectra of GO-P(AM-PVP)

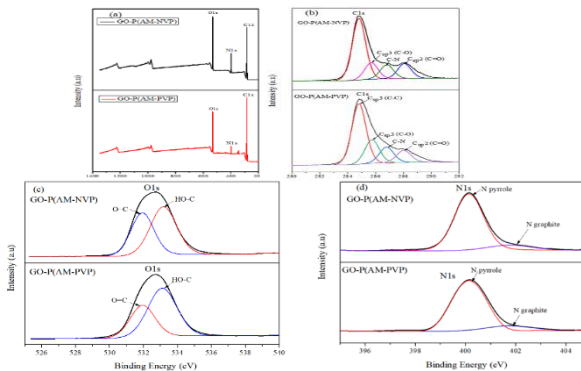


Figure 3.27. XPS spectrum of GO-P(AM-NVP)/ GO-P(AM-PVP)(a) and XPS spectrum of C1s(b), O1s(c), N1s(d) of the two materials.

Fig. 3.27 is the XPS results of GO-P(AM-PVP) and GO(PAM-NVP). The results in Fig.a show that in both spectra, besides the appearance of C1s peak at 285 eV and O1s peak at 532 eV typical for GO, a new peak at 400eV of N1s also appears. The GO-P(AM-NVP) and GO-P(AM-PVP) have the presence of three elements C, O, N, proving that AM-NVP and AM-PVP were successfully attached to GO. The difference in peak intensities in the

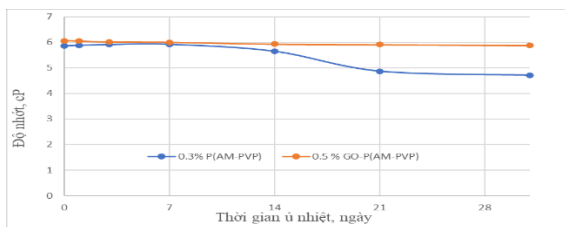
spectral bands of C1s, O1s and N1s of the two materials is due to two different polymerization reaction mechanisms. With the reaction of pre-irradiation to create PVP and then graft AM to create AM-PVP. The peroxides are formed when pre-irradiated PVP. Once the PVP chain is in place, it is clear that pre-irradiation only creates a certain number of peroxide bridges. When polymerizing two monomers by simultaneous irradiation, free radicals can form at the beginning or end of any monomer, oligomer or polymer during the reaction.

### 3.3.4. Applicability of GO-P(AM-PVP) in EOR

\* Evaluation of thermal and chemical resistance of GO-P(AM-PVP)

For application in EOR, all injection solutions, especially polymers, must be able to exist in the reservoir for a long time. Results of evaluating the thermal stability of the material through annealing test at 135 °C for 31 days. Appearance and viscosity of the material after heat annealing are shown in table 3.3.













Table 3.3. and Fig.3.28 shows that the GO-P(AM-PVP) 0.5% wt dispersed in brine annealing at 135 °C for 31 days has an almost unchanged viscosity, proving that the dispersions are stable. Thermal and chemical stability under static conditions are similar to the Miocene and Oligocene reservoirs of WT field.



*Fig.3.28. Graph showing the viscosity of P(AM-PVP) 0.3% wt and GO-P(AM-PVP) 0.5% wt dispersed in brine annealing at 120°C and 135°C according to time*



Table 3.3. Appearance and viscosity of materials P(AM-PVP) 0.3% wt and GO-P(AM-PVP) 0.5% wt after annealing:

Distrib uted system	Annealing time - day/ viscosity -cP					
	0	3	7	14	21	31
P(AM- PVP) 0.3%k l						
	5.56	5.91	5.92	5.65	4.87	5.71
GO- P(AM- PVP) 0.5% kl						
	6.06	6.01	6.0	5.93	5.91	5.88

### CONCLUSIONS AND RECOMMENDATIONS

1. Polymer-coated magnetic nanomaterials - PMNPs - have been synthesized. Physical and chemical characteristics of the material were analyzed by FT-IR, TEM, TGA, XPS, DLS, VSM. The optimal temperature and reaction time of the polymerization of AM-NVP coating on MNPs was found to be 70°C and 8h, the mass of copolymer covering the MNPs surface was 11.04%. The saturation magnetization of PMNPs material is 42 emu/g.
2. Successfully synthesized materials P(AM-NVP) and P(AM-PVP) by direct irradiation method and pre-irradiation method.

- ❖ Finding the optimal irradiation conditions: optimal irradiation dose 5Kgy for P(AM-PVP); 20Kgy for P(AM-PVP) and the optimal AM/NVP monomer ratio is 1.71:1, the monomer concentration is 23.19%.
  - ❖ Finding the optimal irradiation conditions: 5Kgy for P(AM-PVP); 20Kgy for P(AM-PVP) and the optimal AM/NVP monomer ratio is 1.71:1, the monomer concentration is 23.19%.
3. Demonstrate the applicability of PMNPs, GO-P(AM-NVP) and GO-P(AM-PVP) in EOR. PMNPs solution 600ppm, GO-P(AM-NVP) 1.0%wt and GO-P(AM-PVP) 0.5%wt systems are thermally and chemically stable after 31 days of annealing at 120 °C and 135 °C, suitable for applying EOR in offshore reservoirs with high temperature and seawater with high salinity.
- ❖ Proving that 1000 ppm PMNPs nanofluid solution reduces the IFT to 12.4 Nn/m and changes the wettability of reservoir rock from hydrophobic to hydrophilic that increase in oil recovery coefficient.
  - ❖ Proving that the PMNPs nanofluid system has high durability and stability after 4 reuses. This is a material that has potential for practical application to make injection fluid in EOR, contributing to reducing costs.

### **RECOMMENDATIONS**

- ❖ Continue to research and investigate the change in wet adhesion of reservoir rocks of GO-P(AM-NVP) and GO-P(AM-PVP) systems.
- ❖ Injection test of PMNPs, GO-P(AM-NVP) and GO-P(AM-PVP) solutions on Miocene and Oligocene core samples of WT field.
- ❖ Proceed to test injecting material solutions on the pilot.
- ❖ Selection, pilot production and field testing of injection rigs for exploiting PMNPs solution systems, GO-P(AM-NVP) and GO-P(AM-PVP)
- ❖ Proceed to apply three PMNPs solutions, GO-P(AM-NVP) and GO-P(AM-PVP) as injection fluids in reality EOR of the oil and gas exploitation industry.

## LIST OF WORKS HAS BEEN PUBLISHED

1. **Thi-Lieu Nguyen**, Anh-Quan Hoang, Phuong-Tung Nguyen, Anh-Tuyen Luu, Duy-Khanh Pham, Van-Phuc Dinh, Quang-Hung Nguyen, Van-Toan Le, Hai Nguyen Tran, Thi-Bich Luong, *Stable dispersion of graphene oxide-copolymer nanocomposite for enhanced oil recovery application in high-temperature offshore reservoirs*, Colloids and Surfaces A: Physicochemical and Engineering Aspects, 2021, Vol. 628, p. 127343
2. **Thi-Lieu Nguyen**, Anh-Quan Hoang, Duy-Khanh Pham, Hai Bang Truong and Phuong-Tung Nguyen, *Synthesis and evaluation of magnetite nanoparticles coated with (acrylamide-vinylpyrrolidone) polymers on the thermostability for application in harsh offshore reservoirs*, Advances in Natural Sciences: Nanoscience and Nanotechnology, 2023, Vol.14 (2023) 015013 (11pp)
3. **Nguyễn Thị Liễu**, Bạch Thị Mỹ Hiền, Đặng Thị Thu Trang, Nguyễn Văn Lục, Nguyễn Phương Tùng, *Tổng hợp và biến tính vật liệu nano oxit sắt từ ứng dụng trong tăng cường thu hồi dầu*, Tạp chí Khoa học và Công nghệ, Số 49, p 110-117, 2021
4. **Thi-Lieu Nguyen**, Duy-Khanh Pham, Xuan-Truong Mai, Anh-Quan Hoang and Phuong-Tung Nguyen, *Optimized - Polymer - Coated Magnetic Nanoparticles Preparation for use as an Enhanced Oil Recovery Agent*, Proceedings of IWNA 2019, p 227-236, 06 - 09 November 2019.
5. Anh-Quan Hoang, **Thi-Lieu Nguyen**, Anh-Tuyen Luu, Van-Toan Le, Duy-Khanh Pham, Phuong-Tung Nguyen *Graft-polymerization of acrylamide onto pre- polyvinyl pyrrolidone matrix and evaluation of combined copolymer product and graphene oxide nanofluids on the EOR potential in high-temperature offshore oilfields*, Proceedings of IWNA 2023, p 363-367, 08 - 011 November 2023.